InGaN light-emitting diodes with indium-tin-oxide sub-micron lenses patterned by nanosphere lithography

Q. Zhang, K. H. Li, and H. W. Choi[a)]
Department of Electrical and Electronic Engineering, The University of Hong Kong, Hong Kong

(Received 21 December 2011; accepted 23 January 2012; published online 9 February 2012)

Close-packed micro-lenses with dimensions of the order of wavelength have been integrated onto the indium-tin-oxide (ITO) layer of GaN light-emitting diodes employing nanosphere lithography. The ITO lens arrays are transferred from a self-assembled silica nanosphere array by dry etching, leaving the semiconductor layer damage-free. An enhancement of up to 63.5% on optical output power from the lensed light-emitting diode (LED) has been observed. Lens-patterned LEDs are also found to exhibit reduced emission divergence. Three-dimensional finite-difference time-domain simulations performed for light extraction and emission characteristics are found to be consistent with the observed results. © *2012 American Institute of Physics*. [doi:10.1063/1.3684505]

It is well-known that the light extraction efficiency of GaN-based light-emitting diodes (LEDs) is severely restricted due to total internal reflections at the nitride-air interface.[1] One approach for enhancing optical performance of LEDs is the employment of micro-lenses to facilitate extraction of light.[2] Apart from contributing to light extraction, micro-lenses can also be used for modifying directionality of the emitted light.[3] Conventional micro-lens fabrication techniques, such as thermal resist reflow or inkjet printing, allow the formation of micro-lenses of the order of microns.[4–6] Apart from feature dimensions, the packing density of the lens array is also limited since the reflow step requires sufficient spacing between photoresist pedestals of the same scale as the minimum feature sizes.[7] To overcome the limitations of dimension and packing density, nanosphere lithography (NSL) is demonstrated in this work to be capable of patterning close-packed sub-micron lens arrays with scalable dimensions. NSL is also potentially suitable for mass production due to its low set-up costs and high throughput, compared with electron beam or nano-imprint lithography.[8] Previously, monolithic integration of microlenses on the sapphire surface of flip-chip LEDs has been demonstrated.[3] For p-side-up LEDs, processing lenses directly on the p-GaN contact layer may induce plasma damage during dry etching, invariably degrading electrical characteristics of the device;[9] this can be overcome by forming the lenses onto the indium-tin-oxide (ITO) current-spreading layer.

In this letter, we report on the fabrication and characterization of blue InGaN LEDs with integrated ITO lenses whose dimensions are of the order of wavelength or sub-wavelength, patterned by NSL. A monolayer of self-assembled nanospheres serves as an etch mask for pattern transfer onto the ITO layer, resulting in the formation of a hexagonally close-packed ITO lens array after etching. The optical and electrical performances of the packaged devices are evaluated. The finite-difference time-domain (FDTD) method is employed to simulate the optical effects of incorporating ITO lenses with different dimensions to the LEDs.

The LEDs are fabricated according to the process flow illustrated in Figure 1. The InGaN LED wafers are grown on c-plane sapphire substrate by metal-organic chemical vapor deposition (MOCVD), with embedded InGaN/GaN multi-quantum wells designed for emission at around 460 nm. A 200 nm transparent ITO current spreading layer is sputter-deposited. NSL patterning begins with the formation of a self-assembled hexagonal closed-packed monolayer of silica nanospheres by spin coating. The optimized coating conditions have previously been reported.[10] The mean diameters of the spheres used in the work are 195 nm, 310 nm, and 500 nm. For the 195 nm and 310 nm nanospheres, the array directly serves as an etch mask for pattern transfer onto the ITO layer by inductively coupled plasma (ICP) etching. The

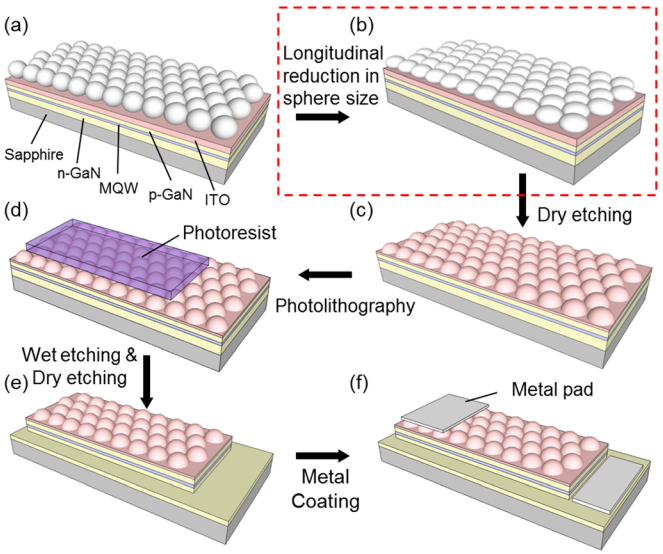

FIG. 1. (Color online) Schematic diagrams showing the fabrication process flow: (a) silica spheres are coated onto the starting LED wafer by spin-coating; (b) additional RIE etching for 500 nm lens to reduce sphere size longitudinally; (c) pattern transfer to ITO layer using ICP etching; (d) mesa definition by photolithography; (e) exposure of n-GaN region by dry etching; (f) metal pads deposition by e-beam evaporation.

[a)]Author to whom correspondence should be addressed. Electronic mail: hwchoi@hku.hk. Tel.: (852) 28572693. Fax: (852) 25598738.

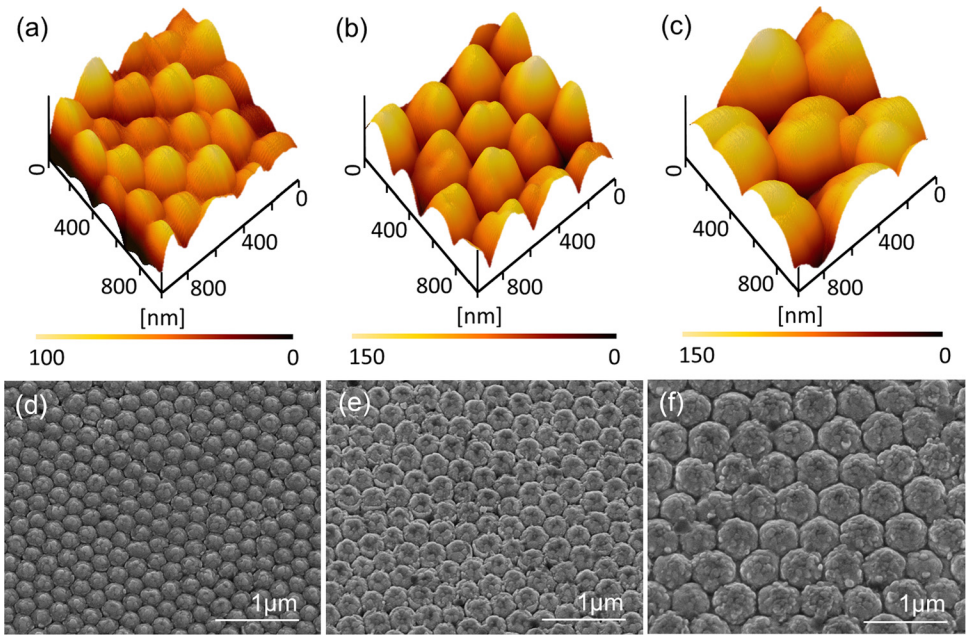

FIG. 2. (Color online) AFM images showing nano-lens with diameter of (a) 195 nm, (b) 310 nm, and (c) 500 nm; FE-SEM images showing nano-lens array in good packing order with diameter of (d) 195 nm, (e) 310 nm, and (f) 500 nm.

coil power and platen power are set to 500 W and 135 W, while the chamber pressure is maintained at 5 mTorr, using a Cl_2 based plasma. The etch duration for all samples is fixed at 180 s so that a 50 nm-thick ITO layer remains beneath the lenses for low-resistivity current spreading. During etching, the spheres themselves shrink both laterally and vertically, transferring onto the ITO layer to become convex lenses. However, with the larger 500 nm spheres, the waists of the spheres remain largely unchanged after 180 s of etching despite a significant reduction in height due to the direction-dependent selectivity, whereby etch rates in the longitudinal direction are much faster than that in the lateral direction, resulting in the formation of GaN pillars with vertical sidewalls. An additional process is thus required prior to ICP etching to shrink the silica spheres longitudinally without etching the GaN layer; this is achieved by selective reactive-ion etching (RIE) using a CHF_3-based plasma under low rf power. At an optimized RIE etch duration of 16 min, the spheres are shaped into olives, whilst remaining closed-packed. The olive-shaped nanospheres can now be transferred onto ITO to become convex lenses. After photolithographic patterning to define a $600 \times 300\,\mu m^2$ mesa, the samples are dry etched to expose the n-GaN layers. The contact pad regions are defined by yet another photolithographic step, followed by e-beam evaporation of the p-pads and n-pads. For comparison, an LED with an un-patterned ITO surface is fabricated alongside. Figures 2(a)–2(c) show surface morphologies of the lenses imaged by atomic force microscope (AFM). Field-emission scanning electron microscopy (FE-SEM) images, as illustrated in Figures 2(d)–2(f), offer a wider view of the same lenses. The heights of the lens structures with diameters of 195 nm, 310 nm, and 500 nm are evaluated to be approximately 100 nm, 150 nm, and 150 nm, respectively. The height of the smallest lens has been intentionally trimmed down to maintain a near-spherical profile and to retain 50 nm of ITO beneath the lenses.

The electrical and optical properties of the lens-patterned LEDs are measured. Figure 3(a) shows the current-voltage (I-V) characteristics of LEDs with and without ITO lenses. The forward voltages for the LEDs with 500 nm, 310 nm, and 195 nm lenses and the unpatterned LED are 3.26 V, 3.24 V, 3.19 V, and 3.19 V, respectively. The series resistances, namely the slopes of the I-V curves in linear region, are almost unchanged. The I-V curves substantiate that structuring of the ITO layer has not degraded the electrical properties of the devices, which would unnecessarily incur resistive losses. Figure 3(b) plots the light output power of LEDs. The light output power of each LED has been measured using a 2×2 cm^2 Si-photodiode placed 2 cm above the emission plane of the LEDs. Compared with the

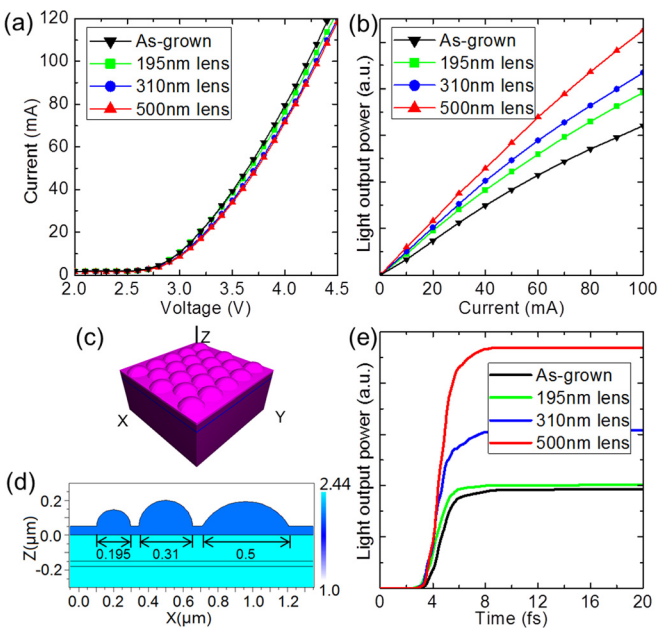

FIG. 3. (Color online) (a) I-V characteristics and (b) light output power as a function of injection current of nano-lens LEDs and as-grown LED; (c) 3D-FDTD constructed nano-lens LED model with diameter of 500 nm; (d) contour map of refractive index with lens profiles; (e) FDTD simulated light output power of nano-lens models and as-grown model.

unpatterned LED, the output powers of LEDs with ITO lenses of 500 nm, 310 nm, and 195 nm diameters have been enhanced by 63.5%, 35.2%, and 22.1% at injection currents of 100 mA, respectively.

To investigate the propagation of light wave in the patterned ITO layer, a three-dimensional FDTD simulation, rigorously solving Maxwell's equation, is carried out. The simulated LED structure emitting at 460 nm is simplified to consist of 200 nm thick ITO/150 nm thick p-GaN/30 nm thick MQWs/1000 nm thick GaN over an area of $4 \times 4\ \mu m^2$. The refractive index of ITO and GaN is set to 2.05 and 2.44. Close-packed plano-convex lenses with diameters of 500 nm, 310 nm, and 195 nm are modeled onto the ITO layer according to the fabricated dimensions, as illustrated in Figure 3(c). A contour map of refractive index for the three modeled lenses is also shown in Figure 3(d). According to the fabricated lens structures, the lens curvatures are not identical. A point radiating source at the center of MQWs is excited continuously so that the light output in all directions can be assumed constant. Only transverse electric (TE)-polarized light is taken into consideration since light emitted from a quantum well sandwiched between two dielectric layers would have a similar polarization.[11] Additionally, experimental results show that TE polarization dominates in GaN-based LEDs.[12] To strike a compromise between computation load and accuracy, the FDTD grid size is set to less than 1/20 of the wavelength, while the time step is set to 0.033 fs to satisfy the Courant stability condition. To calculate all powers extracted from the top of the LED, a large monitor is located closed to the top boundary of the LED model. Figure 3(e) plots the simulated time-dependent light output powers of LED models with and without ITO lenses. All ITO patterned models exhibit enhancement of light output. The largest enhancement of more than 2-fold is observed from the 500 nm lens model. The trend of the simulated results correlates well with that of experimental results, confirming that the 500 nm lens offers better performance than the smaller lenses. The deviation of measured data from the LED with 195 nm lenses may be attributed to non-uniformity of sphere dimensions and loose packing order, since the roughness of the ITO surface becomes comparable to the diameters of the smaller spheres, inducing more point and line defects across the self-assembled sphere array.

Figure 4(a) shows the angular emission profiles of the lens-patterned LEDs operated at 10 mA, measured by rotating a fiber probe coupled to an optical spectrometer around the upper hemisphere of an LED in the range of 0° to 90° in steps of 1°, maintaining a fiber-LED separation of 5 cm. As determined from the normalized polar plots, the full-width-at-half maximum (FWHM) of emission divergence for LEDs with 500 nm, 310 nm, and 195 nm lenses and the unpatterned LED are 94.4°, 111.2°, 114.6°, and 121.2°, respectively. The LED with 500 nm lenses is found to produce the most significant focusing effect with respect to the unpatterned LED, demonstrating a divergence reduction of 26.8° (FWHM), while the changes in divergence from the LEDs with 310 nm and 195 nm lenses are nearly negligible. A three-dimensional FDTD simulation is also conducted to predict the angular emission characteristics of the lens-patterned LEDs. Based on the constructed LED models, point monitors are added to

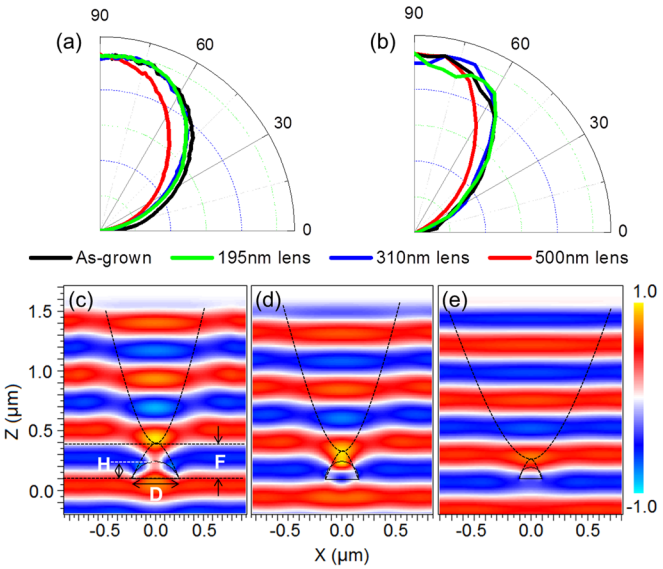

FIG. 4. (Color online) (a) Measured and (b) calculated emission pattern of as-grown LED and nano-lens LEDs (normalized); FDTD simulation results of wave propagating through single lens, $\lambda = 460$ nm, (c) D = 500 nm, H = 150 nm, (d) D = 310 nm, H = 150 nm, (e) D = 195 nm, H = 100 nm.

record the intensity distribution, in steps of 5° in the angular range of 0°–90°; the fixed distance between light source and detector is shortened to $\sim 10\ \mu m$ in order to reduce the computation load. The data collected at each monitor are used to plot the angular emission profiles of the LED models, as shown in Figure 4(b). The simulated results are consistent with the measured data, indicating that only the 500 nm lenses produce a pronounced focusing effect.

To understand this phenomenon, FDTD simulations on individual lenses are conducted. Conventional ray-tracing methods based on Snell's law lose their validity here, since the geometrical dimensions of the lens are of the order of wavelength or even sub-wavelength. In order to depict the focusing behavior clearly, a bundle of parallel rays is employed. Figures 4(c)–4(e) compare the propagation of electromagnetic waves passing through individual lenses of different dimensions; again, the 500 nm lens exhibits the most distinct converging effect. As the lens dimension reduces, the lens focusing effect tends to be weaker, becoming too weak to be observed for the 195 nm lens. The intensity at the focal point of the 195 nm lens is also found to be 1.35 times lower than that from the 500 nm lens. For analysis of lenses with dimensions of the order of wavelength, wave-like features such as interference and diffraction must be taken into consideration. The focusing behavior of lenses with diameters approaching wavelength is a combination of diffraction of waves through lens aperture, diffraction at the lens edges, and complicated interference of waves within the lens itself.[13] As the lens dimension decreases towards sub-wavelength, the extremely high curvature results in a much more tortuous wave pathway than larger lenses to match the phase of the wave within the lens and that outside. It consequently produces a very weak focusing effect and a short focal distance. Additionally, as light emitted from the MQWs of an LED is non-parallel, the converging effect for sub-wavelength lenses becomes even more negligible. Consequently, even though NSL is capable of producing very

small lenses, the minimum dimensions of lenses should not be sub-wavelength.

In summary, the fabrication of GaN LED with ITO lenses via a NSL process has been demonstrated. Significant improvements on light extraction of the lensed LEDs have been observed of up to 63.5% over the bare LED. The LED with 500 nm lenses exhibits a 26.8° reduction in emission divergence (FWHM) compared with the bare LED. The measured data is fully supported with 3D-FDTD simulations on both light extraction and emission characteristics.

This work was supported by a GRF grant of the Research Grant Council of Hong Kong (Project No. HKU 7117/11 E).

[1]A. David, T. Fujii, R. Sharma, K. McGroddy, S. Nakamura, S. P. DenBaars, E. L. Hu, C. Weisbuch, and H. Benisty, Appl. Phys. Lett. **88**, 061124 (2006).
[2]Y. K. Ee, R. A. Arif, N. Tansu, P. Kumnorkaew, and J. F. Gilchrist, Appl. Phys. Lett. **91**, 221107 (2007).
[3]H. W. Choi, C. Liu, E. Gu, G. McConnell, J. M. Girkin, I. M. Watson, and M. D. Dawson, Appl. Phys. Lett. **84**, 2253 (2004).
[4]D. Kim, H. Lee, N. Cho, Y. Sung, and G. Yeom, Jpn. J. Appl. Phys., Part 2 **44**, L18 (2005).
[5]M. Khizar, Z. Y. Fan, K. H. Kim, J. Y. Lin, and H. X. Jiang, Appl. Phys. Lett. **86**, 173504 (2005).
[6]C. H. Tien, C. H. Hung, and T. H. Yu, J. Disp. Technol. **5**, 147 (2009).
[7]P. Nussbaum, R. Volke, H. P. Herzig, M. Eisner, and S. Haselbeck, Pure Appl. Opt. **6**, 617 (1997).
[8]K. H. Li and H. W. Choi, J. Appl. Phys. **109**, 023107 (2011).
[9]H. S. Yang, S. Y. Han, K. H. Baik, S. J. Pearton, and F. Ren, Appl. Phys. Lett. **86**, 102104 (2005).
[10]K. H. Li and H. W. Choi, J. Appl. Phys. **110**, 053104 (2011).
[11]S. H. Fan, P. R. Villeneuve, J. D. Joannopoulos, and E. F. Schubert, Phys. Rev. Lett. **78**(17), 3294 (1997).
[12]J. Shakya, K. Knabe, K. H. Kim, J. Li, J. Y. Lin, and H. X. Jiang, Appl. Phys. Lett. **86**, 091107 (2005).
[13]J. Y. Lee, B. H. Hong, W. Y. Kim, S. K. Min, Y. Kim, M. V. Jouravlev, R. Bose, K. S. Kim, I. C. Hwang, L. J. Kaufman, C. W. Wong, P. Kim, and K. S. Kim, Nature **460**(7254), 498 (2009).